

The Conformation and Activity Relationship of Benzofuran Type of Angiotensin II Receptor Antagonists

Sung-eun Yoo,^{a,*} Soo-Kyung Kim,^{a,c} Sung-Hou Lee,^b Nak-Jung Kim^a and Dai-Woon Lee^c

^aBio-Organic Science Division 5, Korea Research Institute of Chemical Technology, PO Box 107, Yusung-gu, Taejeon 305-606, South Korea

^bScreening Division, Korea Research Institute of Chemical Technology, PO Box 107, Yusung-gu, Taejeon 305-606, South Korea

^cDepartment of Chemistry, Yonsei University, 134 ShinChon-Dong, SeoDaeMoon-Gu, Seoul 120-749, South Korea

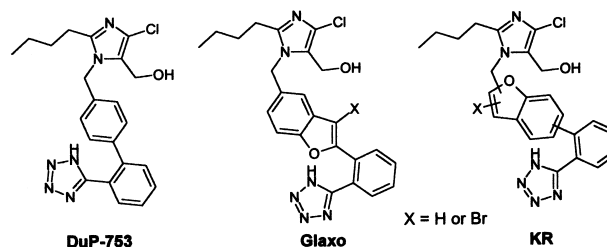
Received 17 April 2000; accepted 5 June 2000

Abstract—As a continuing effort to establish the structure and activity relationship in a benzofuran type of angiotensin II antagonist, we synthesized various regioisomers and performed a series of QSAR analyses. The conformational analyses of target isomers were carried out using molecular mechanics and fine-tuned using the information from the NMR NOE experiment. The conformations of compounds with a good binding activity are quite similar to that of DuP753, a prototype of AII antagonist, suggesting that these compounds also bind to the same site of AII receptor. We then studied the compounds with a varied length of the hydroxyl group bearing side chain to find out the optimum distance between the hydroxyl group and the imidazole ring. The CoMFA with these compounds gave acceptable statistical measures (cross-validated r^2 and conventional r^2 to be 0.881 and 0.974, respectively) and the map was well consistent with the previously proposed pharmacophore. © 2000 Elsevier Science Ltd. All rights reserved.

Introduction

A large number of compounds known as angiotensin II (AII) type I receptor antagonists have been developed for the treatment of hypertension, congestive heart failure and possibly chronic renal failure.¹ Most AII receptor antagonists possess a common structural feature, namely a nitrogen atom, an alkyl chain and an acidic tetrazole group.

In our previous study, we studied to establish the three-dimensional arrangement of pharmacophoric elements for angiotensin II type I receptor antagonists of the benzofuran series (Table 1).² As a continuing effort to establish the QSAR of angiotensin II antagonists, we synthesized additional analogues with different lengths between two key elements, namely the hydroxyl group and the imidazole ring (Table 2, Fig. 1). In addition, we try to explain the discrepancy of the angiotensin II antagonistic activity between the hydrogen-substituted and the bromine-substituted analogues as reported in the Glaxo series.³

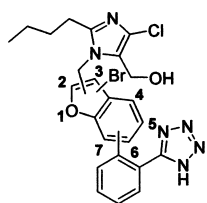


The molecular mechanics based conformational analysis of these compounds was carried out and the resulting low energy conformations were further evaluated with geometrical constraints obtained from the NMR NOE experiment. Then we carried out a series of molecular modeling studies to establish a pharmacophore for the structurally diverse benzofuran analogues. Finally, the comparative molecular field analysis (CoMFA)⁴ was carried out to establish the structural and electronic features of these compounds. A classical QSAR study was also carried out to identify major descriptors which influence the angiotensin II receptor antagonistic activity.

Results and Discussion

The 2D NOESY experiment showed weak NOEs between the protons in the benzofuran ring and those in the butyl

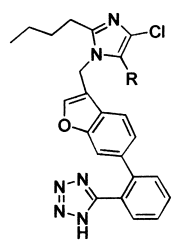
*Corresponding author. Tel.: +82-42-860-7140; fax: +82-42-861-1291; e-mail: seyoo@pado.kRICT.re.kr

Table 1. The angiotensin II antagonistic activities of regioisomers


Compound ^a	The locations of substituents at benzofuran ring			IC ₅₀ (nM)
	Imidazole ring	Tetrazole ring	Br atom	
1	2	5	— ^b	428.54
2	2	5	3	570.04
3	3	6	—	28.3
4	3	6	2	32.34
5	3	5	—	1512.03
6	3	5	2	16,126.96
7	2	6	—	1224.99
8	2	6	3	299.17
9	2	7	—	17,719.84
10	2	7	3	4067.11

^aThe syntheses of these compounds were reported in the previous publication.²

^bThe IC₅₀ for DuP753 is 11.25 nM in our experiments.

Table 2. The angiotensin II antagonistic activities of benzofuran series with various R groups


Compound	R	IC ₅₀ (nM)
3	CH ₂ OH	28.3
11	CH ₂ CH ₂ OH	17.7
12	CH=CHCO ₂ Et	50.6
13	CH=CHCOOH	217.5
14	CH=CHCH ₂ OH	27.7
15	CH ₂ CH ₂ CO ₂ Me	32.7
16	CH ₂ CH ₂ COOH	62.9
17	CH ₂ CH ₂ CH ₂ OH	49.7

side chain or the hydroxymethyl chain (Fig. 2) that is similar to the NOE pattern reported with DuP753.⁵ Since the lowest energy conformer obtained from the random search has a better agreement with NOE experimental data than those from the grid and systematic searches, we used the random search method for a subsequent study.

The lowest energy conformations of **12–17** in Table 2 have hydrogen bondings between the oxygen atoms in the side chain and the nitrogen atoms in the tetrazole ring. However, the best QSAR correlation was obtained when the conformers without internal hydrogen bondings were considered.

Among analogues having different lengths between the hydroxyl group and the imidazole, the best biological activity was observed with the compound **11**, in which

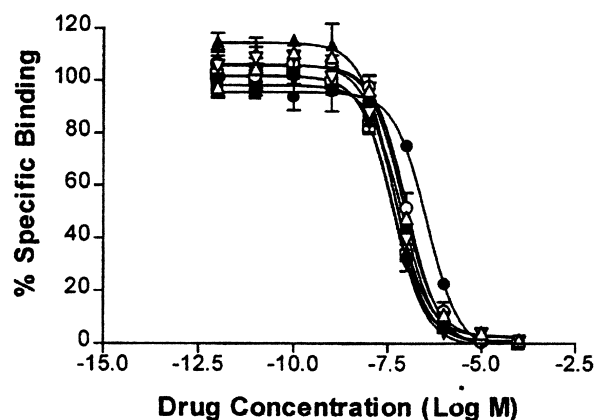
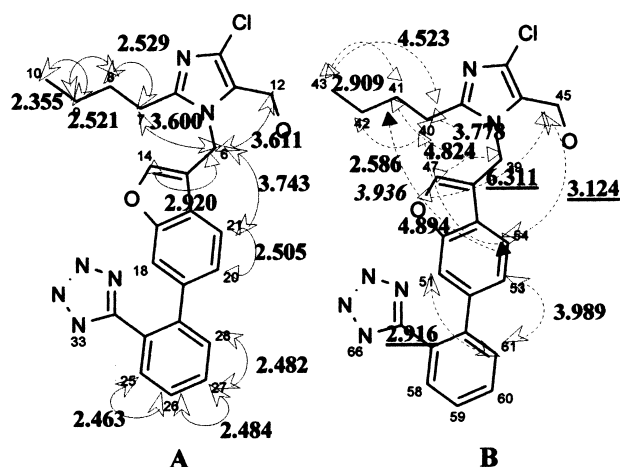


Figure 1. Competition binding curves for human recombinant AII type 1 receptor. All data were obtained in a single experiment, performed in quadruplicate (error bar SEM). Binding is expressed as percentage of specifically bound [¹²⁵I][Sar¹, Ile⁸]-AII. Compound **3** (▲), **11** (□), **12** (△), **13** (●), **14** (▼), **15** (▽), **16** (○), **17** (■).



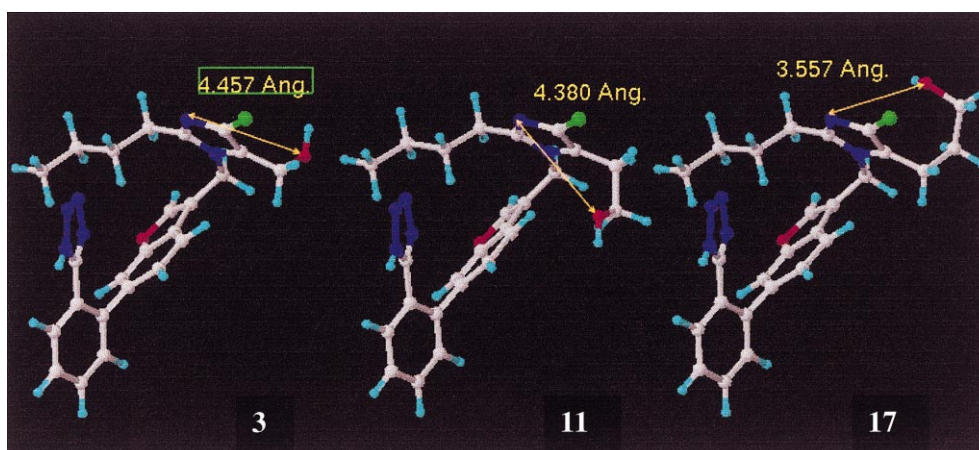


Figure 3. The distances between the nitrogen atom of the imidazole ring and the oxygen atom of the hydroxyl groups (**3**: R = $-\text{CH}_2\text{OH}$, IC_{50} : 28.3 nM; **11**: R = $-\text{CH}_2\text{CH}_2\text{OH}$, IC_{50} : 17.7 nM; **17**: R = $-\text{CH}_2\text{CH}_2\text{OH}$, IC_{50} : 49.7 nM).

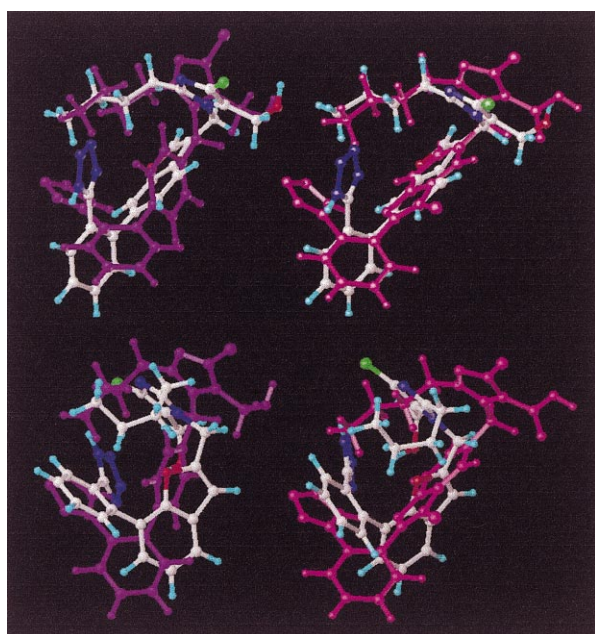


Figure 4. The conformations of the biologically most active and least active compounds of benzofuran series: (top left) the superimposition of the most active compound **3** and the DuP753 compound (purple, rms value: 1.378 Å); (top right) the Glaxo compound (magenta, rms value: 1.164 Å); (bottom left) the superimposition of the least active compound **9** and the DuP753 compound (purple, rms value: 1.829 Å); (bottom right) the Glaxo compound (magenta, rms value: 2.644 Å); the IC_{50} for DuP753 is 11.25 nM in our experiments.

points. On the other hand, in the case of the least active compound **9**, the rmsd values of DuP753 and Glaxo compounds were 1.83 and 2.64 Å and the locations of the tetrazole ring, spacer group and hydroxyl group are notably different from each other (Fig. 4). Thus, the overall conformational similarity between these active conformers was observed, indicating that these active conformers are most likely involved in the same binding site of the receptor.

Previously, Glaxo reported another type of benzofuran derivative and claimed that in their series the bromo-

substituted analogues are generally much more active than the corresponding hydrogen-substituted analogues.⁷ However, in our benzofuran series, we observed all three possible cases: bromo-substituted analogues are less active than the corresponding hydrogen-substituted analogues (**5** versus **6**), similar activities (**3** versus **4**) and more active (**7** versus **8** and **9** versus **10**), respectively. The reason for this activity difference is that the location of bromine atom in the three-dimensional space is quite different from that of GR117289.

Researchers at Glaxo tried to explain this difference initially in terms of the conformational differences between two analogues but later they repropounded that, based on two different crystalline forms of GR117289, it is unlikely that the 3-bromine substitution enhances binding activity by forcing a *cis* relationship between the tetrazole and the benzofuran oxygen atom but by increasing σ -electron withdrawing power of the bromine substituent at the 3 position of the benzofuran ring.⁸

Conformational analysis of our benzofuran series indicated that the bromine substitution did not have any significant effect on conformational changes. Instead, we found that the electronic nature between the hydrogen- and the bromine-substituted analogues was quite different from each other and subsequently dipole moments of the bromine-substituted analogues are larger than those of the hydrogen-substituted analogues. This observation matches well with the conclusion of the Glaxo work for the effect of bromine substitution of benzofuran ring. That is, the substitution of bromine atom effect on the electronic nature not an conformational change through modeling studies. We also found that the direction and the size of dipole moment are correlated well with the binding activity (Fig. 5). For example, the direction of dipole moment of the most active compound **3** (Fig. 5c) is heading toward between the butyl side chain and tetrazole ring. The compounds **1**, **2**, **4** and **8** with IC_{50} less than 600 nM (Table 1) also show similar directions with compound **3**. Especially in the case of compounds **7** and **8**, they have the same three-dimensional structure and the only difference

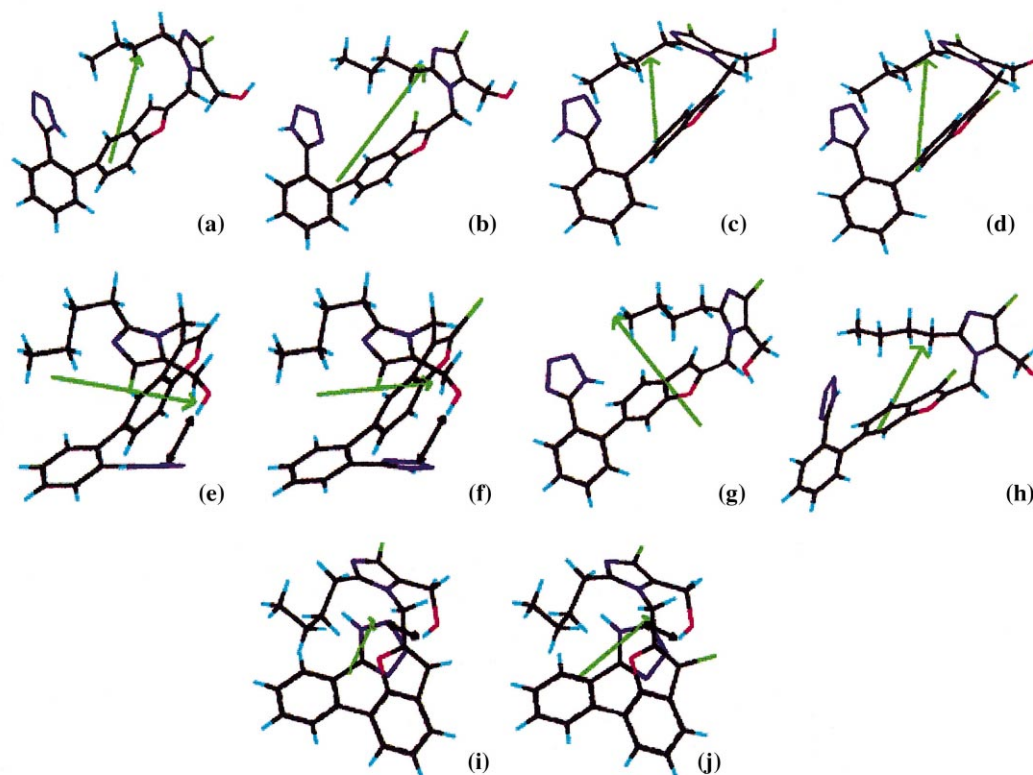


Figure 5. The direction and size of dipole moments for isomers: (a) **1** (DP: 2.91 debye), (b) **2** (DP: 4.22), (c) **3** (DP: 2.94), (d) **4** (DP: 3.62), (e) **5** (DP: 2.25), (f) **6** (DP: 2.35), (g) **7** (DP: 3.28), (h) **8** (DP: 2.47), (i) **9** (DP: 3.38), (j) **10** (DP: 4.04). Green arrow shows dipole moment.

between the two compounds is whether they have a bromine atom or not. However, the activity of compound **8** is 8 times higher than that of compound **7**, and the direction of dipole moment of compound **8** is similar to that of compound **3**.

In our previous report, we indicated that there was some correlation between the binding activity and two distances: between the hydroxyl group and the nitrogen atom at the 3-position in the imidazole ring and the center of the tetrazole ring, respectively.²

Therefore, for QSAR analysis we selected these distances as a descriptor and the RMS deviations in the aforementioned three key elements between our compounds and GR117289. We also included additional descriptors such as shape descriptors and non-shape descriptors and overall 26 descriptors were examined for QSAR analysis.

A simple linear regression showed that a common overlap shape volume (COSV), RMS deviation with GR117289 (ShapeRMS) and F0 value (common overlap shape volume divided by the volume of the individual molecule) were found to be crucial factors for determining the biological activity ($y = 3.8141 + 0.010387 \times \text{COSV}$; $r^2 = 0.72$, $y = 7.42564 + 0.865716 \times \text{ShapeRMS}$; $r^2 = 0.72$, $y = 3.67939 + 4.5946 \times \text{F0}$; $r^2 = 0.71$, when y is $-\log \text{IC}_{50}$). A stepwise multiple regression and genetic function approximation indicated that COSV and ShapeRMS were correlated with binding activities ($y = 4.61592 + 0.009921 \times \text{COSV} + 0.704663 \times \text{ShapeRMS}$; $r^2 = 0.86$, F -test: 42.73, cross-validated $r^2 = 0.77$ for stepwise multiple

regression, $y = 4.61592 + 0.009921 \times \text{COSV} - 0.704663 \times \text{ShapeRMS}$; $r^2 = 0.86$, F -test: 42.73, cross-validated $r^2 = 0.77$ for genetic function approximation).

The plot of variable usage versus number of crossovers showed the frequency of each variable being used in the final equation. Genetic function approximation showed COSV, F0, radiation of gyration, ShapeRMS and the distances between the center of tetrazole and the nitrogen atoms in imidazole ring survived by evolving random initial models using a genetic algorithm (Fig. 6).

A set of 17 compounds, of which activity (IC_{50}) values ranged over 3 orders of magnitude as shown in Tables 1 and 2, were selected for the CoMFA analysis. Instead of using the lowest energy conformers with internal hydrogen bondings as mentioned previously, we used the next lowest energy conformers having no internal hydrogen bondings. The result of the CoMFA analysis for 17 training sets is summarized in Table 3. The CoMFA analysis shows a good correlation with cross-validated r^2 and conventional r^2 to be 0.881 and 0.974, respectively, after removing two outliers.

The CoMFA map displays a pharmacophore which is quite consistent with that of AII antagonists reported by us⁹ and others¹⁰ (Fig. 7). The results from three-dimensional and classical QSAR analyses will provide useful information for understanding the structural and electrostatic requirements necessary for a good angiotensin II receptor antagonist and will be useful in designing effective novel antagonists.

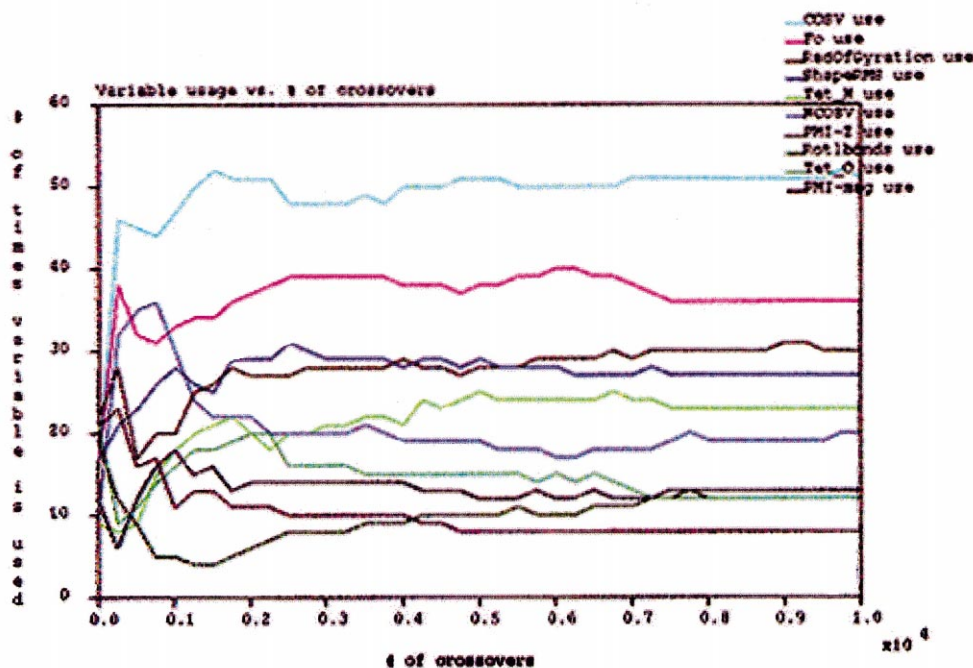


Figure 6. The plot of variable usage versus number of crossovers. The order of variables in top right shows the frequency of descriptor when evolving random initial models using a genetic algorithm. The higher number of variable usage with the increase of the number of crossovers means that the descriptor is important in the model.

Table 3. Summary of CoMFA-PLS results

	Model 1	Model 2
Cross-validated r^2	0.869	0.881
No. of component	2	2
r^2	0.974	0.973
Standard error of estimate	0.162	0.165
F values	221.91	214.60
Steric (%)	49.7	51.2
Electrostatic (%)	50.3	48.8
Region focusing	X	O

Methods

Biological data

Binding assays were quadruplicated and performed in 96-well plates by incubating aliquots of the human recombinant AII receptor subtype I (BioSignal Inc., Canada) with 0.21 nM of [125 I][Sar¹, Ile⁸]-AII. Test compounds were dissolved at 2.5 mM in dimethylsulfoxide and serially diluted to nine concentrations for the activity screening in total assay volume of 250 μ L. The assay buffer contained 50 mM Tris, 5 mM MgCl₂, 1 mM EDTA, 0.1% bovine serum albumin (pH 7.4). Specific [125 I][Sar¹, Ile⁸]-AII binding was determined experimentally from the difference between counts in the absence and presence of 10 μ M unlabeled.

After incubation at 37 °C for 60 min, the incubation mixtures were filtered through glass-filter GF/C filters (Wallac, Finland) which were presoaked in 0.3% polyethylenimine and rapidly washed nine times with 200 μ L of ice cold 50 mM Tris buffer (pH 7.4) using the Inotech harvester (Inotech, Switzerland). The filters were covered with MeltiLex (melted on scintillator, Wallac, Finland),

sealed in sample bag followed by drying in the oven, and counted by MicroBeta (Wallac, Finland). The ability of antagonists to inhibit specific [125 I][Sar¹, Ile⁸]-AII binding was estimated by IC₅₀ values, which are the molar concentrations of unlabeled drugs necessary to displace 50% of specific binding. The value for K_i was calculated from the equation (relationship between the inhibition constant (K_i) and the concentration of inhibitor which causes 50% inhibition (IC₅₀) of an enzymatic reaction) $K_i = \text{IC}_{50}/(1 + L/K_d)$, where L equals the concentration of [125 I][Sar¹, Ile⁸]-AII.¹¹ The data from binding experiments were analyzed by nonlinear regression, using the PRISM computer program (GraphPad Software Inc., San Diego, CA).

NMR experiments

Samples for the NMR studies were prepared in CD₃OD. All NMR experiments were performed using a Bruker 600 MHz spectrometer at 25 °C. Mixing times of 250 and 400 ms for NOESY were used.

Molecular modeling

All molecular modeling and QSAR studies described herein were performed on Silicon Graphics workstations using the SYBYL (v. 6.4 from Tripos, Inc., St. Louis, MO) and Cerius2 (v. 3.5 from MSI).

A set of 17 compounds with specific biological activity (IC₅₀) values ranging over 3 orders of magnitude were used (Tables 1 and 2). All compounds were energy-minimized with the Tripos force field¹² with a distance-dependent dielectric function and a 0.05 kcal/mol energy gradient convergence criterion. Partial atomic charges

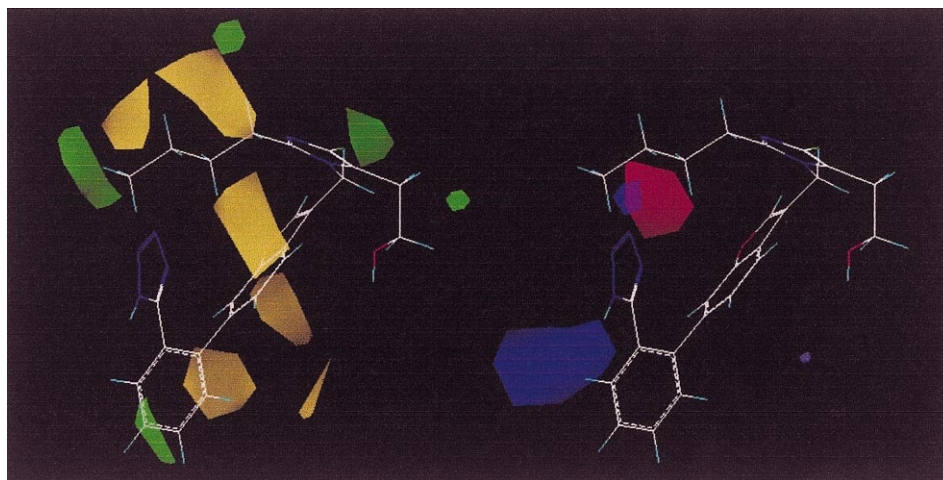


Figure 7. The CoMFA contour maps of benzofuran series: (left) steric contour: for steric contours increased binding results from placing bulkier group near green and less bulkier group near yellow; (right) electrostatic contour: for electrostatic contours increased binding results from placing more positive (+) charge near blue and negative (–) charge near red. The most active compound **11** in benzofuran series is shown.

required for calculation of the electrostatic interaction energies were calculated by using the Gastieger–Marsili method.¹³ The lowest energy conformers were obtained by the random search. The database of molecules, the training set, was suitably aligned in three-dimensional space according to manual fitting with key atoms of known pharmacophore. The CoMFA analysis was performed using the QSAR module of Sybyl with the molecules embedded in a regularly spaced (2.0 °C grid box of 18×20×22 °C) (these values were determined by an automatic procedure performed by the Sybyl-CoMFA routine). Steric and electrostatic interaction energies were calculated using sp³ carbon probes with a +1 charge. After constructing the field, steric and electrostatic fields were calculated for each molecule by interacting with a probe atom at every grid point surrounding the aligned database in three-dimensional space. To correlate these field energy terms with their AII antagonistic activities, partial least squares (PLS) analysis¹⁴ was used with cross-validation, giving a measure of the predictive power of the model. The final PLS analysis was then performed using no cross-validation with an optimum number of components reported from the cross-validation results. The steric and electrostatic fields were scaled according to CoMFA standard deviation in order to give the same potential weights on the resulting QSAR.

For a classical QSAR analysis, we performed molecular shape analysis first to obtain shape descriptors and then added other non-shape descriptors. QSAR is optimized using various statistical methods such as simple linear regression, stepwise multiple linear regression, partial least squares and genetic function approximation.¹⁵

Acknowledgements

We thank the Center for Molecular Design and Synthesis at KAIST for financial support and Tripos Associates for providing us with the SYBYL program.

References and Notes

- Wexler, R. R.; Greenlee, W. J.; Irvin, J. D.; Goldberg, M. R.; Prendergast, K.; Smith, R. D.; Timmermans, P. B. M. W. M. *J. Med. Chem.* **1996**, *39*, 625.
- Yoo, S. E.; Lee, S. H.; Kim, S. K.; Lee, S. H. *Bioorg. Med. Chem.* **1997**, *5*, 445.
- Robertson, M. J.; Barnes, J. C.; Drew, G. M.; Clark, K. L.; Marshall, F. H.; Michel, A.; Middlemiss, D.; Ross, B. C.; Scopes, D.; Dowle, M. D. *Br. J. Pharmacol.* **1992**, *107*, 1173.
- Cramer, R. D. III; Patterson, D. E.; Bunce, J. D. *J. Am. Chem. Soc.* **1988**, *110*, 5959.
- Mavromoustakos, T.; Kolocouris, A.; Zervou, M.; Roumelioti, P.; Matsoukas, J.; Weisemann, R. *J. Med. Chem.* **1999**, *42*, 1714.
- Duncia, J. V.; Carini, D. J.; Chiu, A. T.; Johnson, A. L.; Price, W. A.; Wong, P. C.; Wexler, R. R.; Timmermans, P. B. M. W. M. *Med. Res. Rev.* **1992**, *12*, 149.
- Middlemiss, D.; Drew, G. M.; Ross, B. C.; Robertson, M. J.; Scopes, D. I. C.; Dowle, M. D.; Akers, J.; Cardwell, K.; Clark, K. L.; Coote, S.; Eldred, C. D.; Hamblett, J.; Hilditch, A.; Hirst, G. C.; Jack, T.; Montana, J.; Panchal, T. A.; Paton, J. M. S.; Shah, P.; Stuart, G.; Travers, A. *Bioorg. Med. Chem. Lett.* **1991**, *1*, 711.
- Middlemiss, D.; Watson, S. P. *Tetrahedron* **1994**, *50*, 13049.
- Yoo, S. E.; Shin, Y. A.; Lee, S.-H.; Kim, N.-J. *Bioorg. Med. Chem.* **1995**, *3*, 289.
- Duncia, J. V.; Chiu, A. T.; Carini, D. J.; Gregory, G. B.; Johnson, A. L.; Price, W. A.; Wells, G. J.; Wong, P. C.; Calabrese, J. C.; Timmermans, P. B. M. W. M. *J. Med. Chem.* **1990**, *33*, 1312.
- Cheng, Y.; Prusoff, W. H. *Biochem. Pharmacol.* **1973**, *22*, 3099.
- Clark, M. D.; Cramer, R. D. III; Opdenbosch, N. V. *J. Comput. Chem.* **1980**, *10*, 982.
- Gasteiger, J.; Marsili, M. *Tetrahedron* **1980**, *36*, 3219.
- (a) Glen, W. G.; Dunn, W. J. III; Scott, D. R. *Tetrahedron Computer Methodology* **1989**, *2*, 349. (b) Stahle, L.; Wold, S. *Progr. Med. Chem.* **1988**, *25*, 292.
- Rogers, D.; Hopfinger, A. J. *J. Chem. Inf. Comput. Sci.* **1994**, *34*, 1297.